Two-Dimensional Material Response of a Transpiration-Cooled System in a Radiative/Convective Environment

Izumi Ishii* and Hirotoshi Kubota†
University of Tokyo, Tokyo, Japan

The two-dimensional unsteady material response of a transpiration-cooled system in a radiative/convective heating environment is analyzed numerically with the use of the strongly implicit procedure (SIP). The internal mass flow rate, internal pressure, and in-depth solid and fluid temperature distributions are obtained for various matrix porosities and coolant mass injection rates in a CO_2/silica transpiration-cooled system. The results for application on Saturn entry vehicles provide a feasible idea for a thermal protection system in a severe radiative/convective heating environment. The feasibility of this analysis is tentatively verified by comparison with the experimental results of a radiation simulation of one-dimensional, relatively low-incident radiative heating.

Nomenclature

C_p = specific heat
h_v = volumetric convective heat-transfer coefficient
I_e = external incident radiative intensity
I_R = radiation intensity outward in the matrix
I_T = radiation intensity transmitted inward in the matrix
K = absorption coefficient
k = thermal conductivity
L_x, L_y = dimension in the x and y directions
m_{ref} = reference mass injection rate
m, m' = index on radiation bands that penetrate the matrix
n, n' = index on radiation bands absorbed on the exposed surface
p = pressure
Q = heat flux
R = gas constant
S = scattering coefficient
T = temperature
t = time
u, v = components of superficial velocity
v = superficial velocity vector
x, y = space coordinates
$\tilde{\alpha}$ = viscous coefficient
$\tilde{\beta}$ = inertial coefficient
ϵ = emissivity
η = reflectivity
μ = viscosity
ρ = density
σ = Stefan-Boltzmann constant
ϕ = porosity
ψ_1 = radiative heat-transfer correction factor due to mass injection
ψ_2 = convective heat-transfer correction factor due to mass injection

Subscripts

b = back face
c = convective
e = external
f = fluid
i = internal
r = radiative
rerad = reradiative
s = solid
w = wall (surface)
ν = νth spectral band of radiation
0 = without mass injection

Received Jan. 14, 1983; revision received Aug. 18, 1983.

*Graduate Student, Department of Aeronautics, Faculty of Engineering (presently, with Mitsubishi Heavy Industries, Ltd., Nagoya, Japan).

†Associate Professor, Department of Aeronautics, Faculty of Engineering. Member AIAA.

Introduction

THERE are many practical fields of mechanical, chemical, and aerospace engineering where radiative/convective heating must be deduced. One application in the aerospace field, for example, is a probe with an ablative thermal protection system[1,2] that enters the atmosphere of a giant outer planet and encounters severe radiative heat loads in association with convective heat loads. In such an environment, the ablation-cooled system is a very effective method of thermal protection, including the effects of reduction of convective heating by mass injection into the boundary layer, of heat release by phase change of the surface material, and of radiation absorption by the ablated gas species.

Another approach to thermal protection is a transpiration-cooled system. This system has some deficiencies compared with the ablation-cooled system, such as auxiliary subsystem complexity, troublesome maintenance, structural weakness, etc. However, if it is used appropriately, it is expected that transpiration cooling will be more effective in the radiative/convective heating environment than the simple ablation system. The transpired gas decreases the convective heating and the porous matrix itself partially reflects the incident radiative heat flux, while a coolant gas flowing through the matrix partially absorbs the radiation and transports it out of the matrix. Heat exchange between the matrix and the coolant gas is also beneficial.

The analytical studies for such a transpiration-cooled system were performed by Kubota for both quasisteady and unsteady cases under a one-dimensional assumption[3,4] and for coupling with ablation.[5] The advantage of the coupled transpiration-cooled system over the simple ablation-cooled system is also discussed in Ref. 5. However, these discussions are for a one-dimensional case, and a multidimensional thermal analysis is required for a complete estimation of the cooling effectiveness.

Many investigations concerning the flow through porous media reveal that the Darcy law is consistent for such a flow condition. Curry[6] predicted the heat and mass transfer in a two-dimensional porous matrix heated convectively by solving the modified Darcy equation, an energy equation for the fluid, and an energy equation for a solid matrix with the use of the strongly implicit procedure (SIP).[7] This implicit

scheme was successfully applied to the solution of a system of coupled, nonlinear partial differential equations.

The objectives of the present paper are to analyze the two-dimensional flow characteristics within the porous matrix, subject to the radiative/convective heat loads with the use of SIP, by adding the radiative transfer term to the analysis of Ref. 6 and to estimate the thermal protection effectiveness of this transpiration-cooled system. Special attention is given to the radiative transfer within a matrix consisting of a reflecting solid and the absorbing fluid. It can show how to treat such a system and provide a feasible idea for a thermal protection system.

Mathematical Model and Assumptions

The mathematical model is sketched in Fig. 1. The dimensions of the porous matrix are L_x and L_y, respectively. The coolant fluid enters at the back face $x=L_x$ with a reference mass injection rate m_{ref} and flows toward the front surface $x=0$. The incident radiative and convective heats $Q_{r_e}(y)$ and $Q_c(y)$ and the external pressure $p_e(y)$ are specified. The analysis assumes that the solid and fluid temperatures are not equal and that there is no reversal flow, chemical reaction within the matrix, or melting of the material.

Governing Equations

A set of governing equations for the two-dimensional, unsteady heat and mass transfer reduced by Curry[6] is rewritten by adding a radiative transfer term to the energy equations, as follows for the fluid:

Darcy's continuity

$$\frac{\phi}{p_f}\frac{\partial}{\partial t}\left(\frac{p_f^2}{T_f}\right)-\frac{\partial}{\partial x}\left[\frac{1}{T_f(\tilde{\alpha}\mu_f+\tilde{\beta}\rho_f|v_f|)}\frac{\partial p_f^2}{\partial x}\right]$$

$$-\frac{\partial}{\partial y}\left[\frac{1}{T_f(\tilde{\alpha}\mu_f+\tilde{\beta}\rho_f|v_f|)}\frac{\partial p_f^2}{\partial y}\right]=0 \tag{1}$$

energy conservation

$$C_{pf}\rho_f\left(\frac{\partial T_f}{\partial t}+\frac{u_f}{\phi}\frac{\partial T_f}{\partial x}+\frac{v_f}{\phi}\frac{\partial T_f}{\partial y}\right)=\frac{\partial}{\partial x}\left(k_f\frac{\partial T_f}{\partial x}\right)$$

$$+\frac{\partial}{\partial y}\left(k_f\frac{\partial T_f}{\partial y}\right)+\frac{h_v}{\phi}(T_s-T_f)-\nabla Q_r \tag{2}$$

perfect-gas law

$$p_f=\rho_f R T_f \tag{3}$$

Darcy's pressure drop

$$-\nabla p_f=(\tilde{\alpha}\mu_f+\tilde{\beta}\rho_f|v_f|)v_f \tag{4}$$

and for the solid:

energy conservation

$$C_{ps}\rho_s\frac{\partial T_s}{\partial t}=\frac{\partial}{\partial x}\left(k_s\frac{\partial T_s}{\partial x}\right)+\frac{\partial}{\partial y}\left(k_s\frac{\partial T_s}{\partial y}\right)$$

$$-\frac{h_v}{1-\phi}(T_s-T_f)-\nabla Q_r \tag{5}$$

The matrix material is partially transparent to radiation so that a part of the incident radiative heat flux penetrates the matrix to be backscattered in depth and the rest is absorbed at the surface. The incident radiation is defined as[8]

$$Q_{r_e}=\sum_{\nu=m}^{m'}Q_{r_{e_\nu}}+\sum_{\nu=n}^{n'}Q_{r_{e_\nu}} \tag{6}$$

where the first and the second terms on the right-hand side represent the radiative heat that penetrates and is absorbed at the surface, respectively, for the frequency ν of m through m' and n through n'. Thus, the radiative heat flux within the matrix Q_r should be evaluated under the influence of the penetrating incident radiative flux

$$\sum_{\nu=m}^{m'}Q_{r_{e_\nu}}$$

The radiative transfer within the matrix is assumed to be one-dimensional in spite of the two-dimensionality of fluid mechanics, because the x-wise radiative transfer is dominant in uniform incident radiative heating. Hence, by the "two-flux" method described in the Appendix, it is written, by neglecting volumetric emission, as

$$Q_r=\sum_{\nu=m}^{m'}Q_{r_{e_\nu}}=\sum_{\nu=m}^{m'}\pi(I_{T_\nu}-I_{R_\nu}) \tag{7}$$

The radiative term ∇Q_r in Eqs. (2) and (5) is the same for the solid and the fluid, because it consists of a common absorbed coefficient and a common scattering coefficient weighted by porosity on the respective properties [see Eqs. (A3) and (A4) in the Appendix]. From the solution of the Kubelka-Munk equations (A1) and (A2), it is then expressed in a one-dimensional form by

$$\frac{dQ_r}{dx}=\sum_{\nu=m}^{m'}\pi\left(\frac{dI_{T_\nu}}{dx}-\frac{dI_{R_\nu}}{dx}\right)=-\sum_{\nu=m}^{m'}\pi K(I_{T_\nu}+I_{R_\nu})$$

$$=-2\left(\frac{A_0}{A_1}\right)e^{\alpha x}K\sum_{\nu=m}^{m'}Q_{r_{e_\nu}}+2\left(\frac{B_0}{B_1}\right)e^{-\alpha x}K\sum_{\nu=m}^{m'}Q_{r_{e_\nu}} \tag{8}$$

Boundary and Initial Conditions

The boundary conditions are specified according to the mathematical model shown in Fig. 1.

At $x=0$ (front surface):

(Heat flux conducted inside the matrix)

= (incident radiative heating absorbed at the surface)

+ (incident convective heating)

− (reradiative heat flux outward the matrix)

or

$$-k_s\frac{\partial T_s}{\partial x}=\psi_1\sum_{\nu=n}^{n'}Q_{r_{e_\nu}}+\psi_2 Q_c-Q_{\text{rerad}} \tag{9}$$

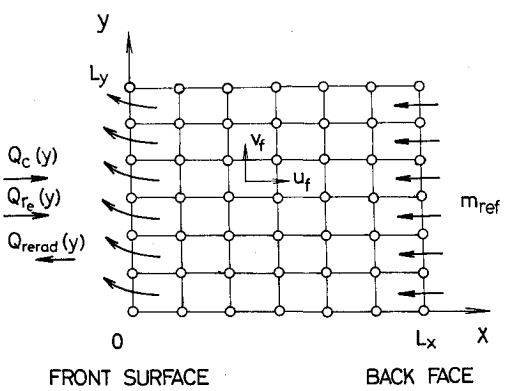

Fig. 1 Mathematical model.

Table 1 Properties of porous silica

Property	Value at 1981 K	Value at 300 K	Dimension	Ref.
k_s	2.290	0.903	W/m·K	8
C_{p_s}	1.294	0.720	kJ/kg·K	8
ρ_s	1.49×10^3	1.49×10^3	kg/m^3	8
K_s	0.001	0.001	1/cm	8
S_s	40	40	1/cm	8
η_e	0.06511	0.06511		8
η_i	0.17	0.17		8
η_b	0.8	0.8		8
ϵ	0.14	0.14		10

Table 2 Properties of carbon dioxide

Property	Value at 1981 K	Value at 300 K	Dimension	Ref.
k_f	0.1458	0.999×10^{-2}	W/m·K	11
C_{p_f}	1.369	0.846	kJ/kg·K	12
K_f	0.1172	0.1172	1/cm	13
S_f	0	0	1/cm	13
μ_f	5.99×10^{-5}	1.50×10^{-5}	Pa·s	11

where $Q_{\text{rerad}}=\sigma\epsilon T_s^4$, and ψ_1 and ψ_2 represent how many incident radiative and convective heatings are blocked due to the transpired gas in an external flow out of the matrix,

$$\frac{\partial^2 T_f}{\partial x^2}=0 \tag{10}$$

$$p_f=p_e \tag{11}$$

At $x=L_x$ (back face):

$$T_s=T_f=T_b=\text{const} \tag{12}$$

At the back face, the mass flow rate has a constant value of m_{ref}.

Two x-directional boundary conditions for pressure are necessary because the differential of Darcy's continuity equation (1) is of second order. While the pressure is specified at the front surface, either the pressure or pressure gradient must be given at the back face. Two kinds of boundary condition for the back-face pressure are considered, that is,

$$\text{Case A:}\quad \frac{\partial p_f}{\partial x}=0 \tag{13}$$

$$\text{Case B:}\quad \frac{\partial p_f^2}{\partial x}=-2RT_b(\tilde{\alpha}\mu_f+\tilde{\beta}m_{\text{ref}})m_{\text{ref}} \tag{14}$$

The boundary condition for case A is the same as one proposed by Curry,[6] which sets an impermeable seal on the injection zone. When this boundary condition is used, ∇p_f equals 0 at $x=L_x$; hence, from Eq. (4), $(\tilde{\alpha}\mu_f+\tilde{\beta}\rho_f|v_f|)_{x=L_x}=0$. This leads to $\tilde{\alpha}\mu_f+\tilde{\beta}m_{\text{ref}}=0$ at the back face, where the reference mass injection rate m_{ref} cannot be given arbitrarily but is an eigenvalue, because other properties such as $\tilde{\alpha}$, $\tilde{\beta}$, and μ_f are constant for an isothermal (constant temperature in the matrix) case. The boundary condition for case B, using the equations of Darcy's pressure drop and perfect gas just at the back face, excludes the above limitation and can give the solutions for the various reference mass injection rates.

At $y=0$ and L_y, symmetric boundaries are assumed in the y direction,

$$\frac{\partial T_s}{\partial y}=\frac{\partial T_f}{\partial y}=\frac{\partial p_f}{\partial y}=0 \tag{15}$$

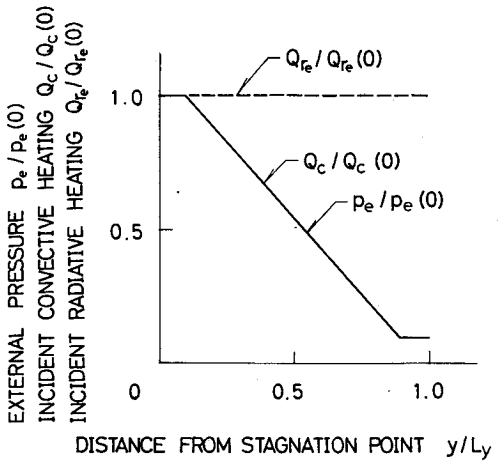

Fig. 2 Boundary conditions at front surface.

and at $t=0$,

$$T_s=T_f=T_b, \qquad p_f=p_e \tag{16}$$

Results and Discussion

The governing equations are normalized by using appropriate nondimensionalization and solved numerically with the use of the SIP scheme under the normalized boundary and initial conditions. The detailed descriptions on the method of solution are in Ref. 9.

Representative calculations were performed for the CO_2 transpiration through a silica (SiO_2) porous matrix for application to Saturn entry. SiO_2 and CO_2 were chosen as a radiative reflecting porous solid and a radiative absorbing coolant gas. The two-dimensional calculation can be applied to a one-dimensional case by making the y coordinate degenerate. An example is verification of the experimental result from the radiation simulation of a one-dimensional, relatively low heating condition.

The thermal and optical properties listed in Tables 1 and 2 were used in these calculations. Since the fluid mechanical properties of porous silica are not available, the experimental correlation for porous felt metal[14] and sintered metal[15] used were

$$\tilde{\alpha}=0.734\times10^9(100\phi)^{-1.538}\text{cm}^{-2}$$

$$\tilde{\beta}=0.152\times10^4(100\phi)^{0.252}\text{cm}^{-1}$$

and

$$h_v=0.00434(C_{p_f}k_f^2)^{0.333}\mu_f^{-0.227}(\rho_f|v_f|)^{0.56}(\tilde{\alpha}/\tilde{\beta})^{1.44}$$

Case 1

The radiative and convective heatings for this sample calculation are taken for a 15 deg Saturn entry[8] at $t=23.7$ s corresponding to the maximum radiative heat loads. The distributions of the incident convective heat load $Q_c(y)$ and the external pressure $p_e(y)$ are specified as illustrated in Fig. 2, where $Q_c(0)=545$ W/cm^2 and $p_e(0)=0.21$ N/cm^2 at the stagnation point. The incident radiative heating Q_{r_e} is assumed to be independent on the y coordinate and is 263 W/cm^2 (161.6 W/cm^2 for the penetrating radiating heating and 101.4 W/cm^2 for the surface-absorbed radiating heating). The initial and the back-face temperatures are fixed at 300 K. All calculations were carried out for the sample case of $\psi_1=\psi_2=1$, which means that the incident radiative and convective heatings are not influenced by the mass injection. The matrix thickness L_x is 1.0 cm.

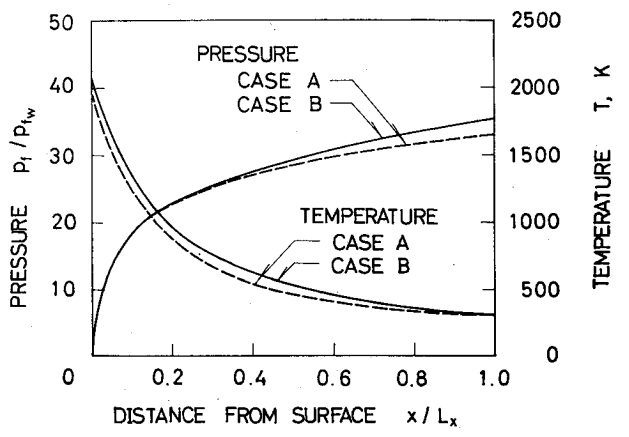

Fig. 3 Internal pressure and in-depth solid temperature ($m_{ref} = 0.07$ g/cm^2·s, $\phi = 0.66$, $y/L = 0.0$, $t = 30$ s).

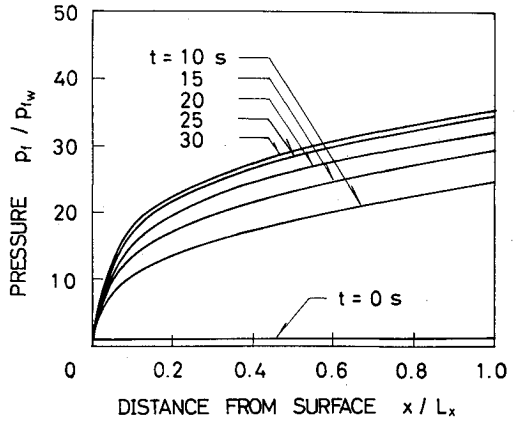

Fig. 4 Unsteady internal pressure ($m_{ref} = 0.07$ g/cm^2·s, $\phi = 0.66$, $y/L = 0.0$).

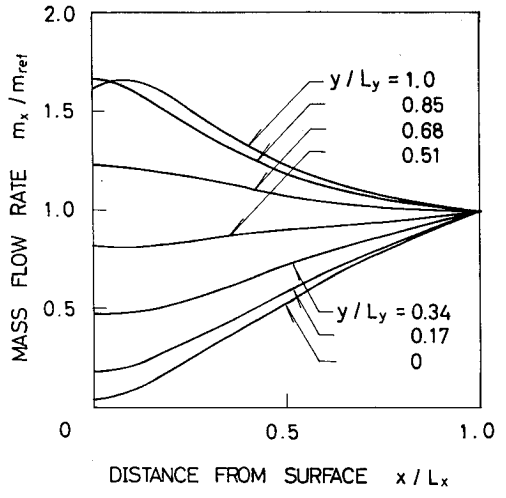

Fig. 5 Internal mass flow rate normal to surface ($m_{ref} = 0.1$ g/cm^2·s, $\phi = 0.66$, $t = 30$ s).

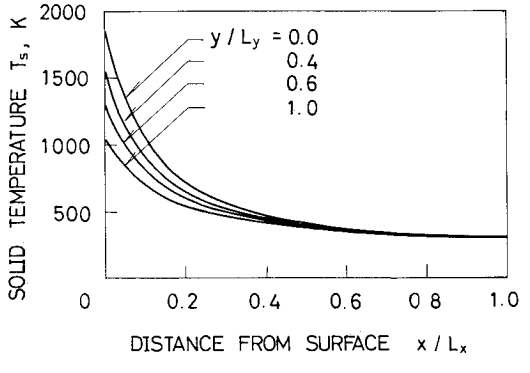

Fig. 6 Solid temperature within porous matrix ($\phi = 0.66$, $t = 30$ s).

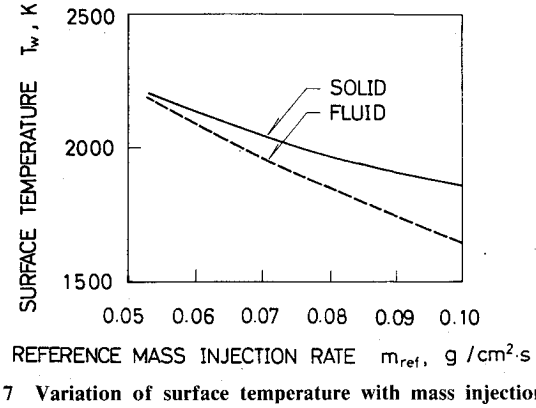

Fig. 7 Variation of surface temperature with mass injection rate ($\phi = 0.66$, $y/L = 0.0$, $t = 30$ s).

Figure 3 shows profiles of the internal pressure and the in-depth solid temperature for $m_{ref} = 0.07$ g/cm^2·s for the different boundary conditions A and B. As some discrepancy is seen between them, case B is used for the following calculation for the reason described in the previous section. Although it seems that the back-face pressure is exaggeratedly high, the actual back-face pressure has a reasonable value for the small external pressure of 0.21 N/cm^2. Figure 4 represents the unsteady characteristics of the internal pressure, which is almost saturated in 20-30 s.

A typical internal mass flow rate normal to the surface m_x/m_{ref} is shown in Fig. 5 for $m_{ref} = 0.1$ g/cm^2·s at $t = 30$ s, which indicates the greater number of coolant mass flows outward ($y/L_y \to 1.0$) due to the higher external pressure at the stagnation point ($y/L_y = 0.0$). The corresponding in-depth solid temperatures are demonstrated in Fig. 6, showing the highest temperature at the stagnation point. The surface solid and fluid temperatures with the various mass injection rates are illustrated in Fig. 7. When cooling effectiveness is defined as the rate of the decrease in the surface solid temperature per mass injection rate, it may perhaps have a lower value as the mass injection rate increases (in spite of the fact that the surface solid temperature itself decreases), because the rate of temperature decrease becomes small for the increase of the mass injection rate. The lower porosity increases the cooling effectiveness because of the greater pore velocity as shown in Fig. 8.

Increasing the incident radiative heating Q_{r_e}, while keeping the incident convective heating constant, may raise the levels of the in-depth solid temperatures and also of the surface solid temperatures. These effects are demonstrated in Figs. 9 and 10. In Fig. 9, the nondimensional in-depth solid temperature $(T_s - T_b)/(T_{s_w} - T_b)$ is shown to be higher for greater incident radiative heating. This means that the penetrating radiative heat load also raises the matrix temperature. The solid line in Fig. 10 represents the surface solid temperature, while the dashed line shows the radiation equilibrium temperature that can be estimated when the left-hand side of Eq. (9) is equal to zero. The difference of both curves is considered to be the advantage of mass transpiration. The surface solid temperature with mass transpiration increases but gradually saturates as the radiative heating increases. This is the desirable characteristic for a thermal protection system in an environment of severe radiation.

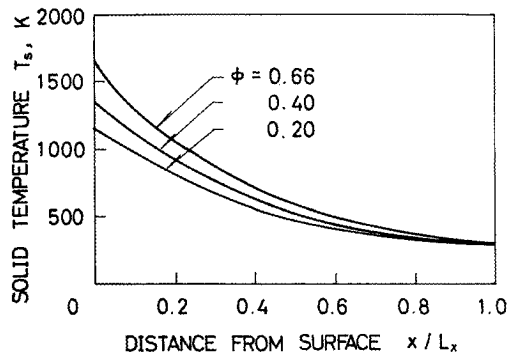

Fig. 8 Effect of porosity ($m_{ref}=0.1$ g/cm^2·s, $Q_{r_e}=263$ W/cm^2, $Q_c=54.5$ W/cm^2, $y/L=0.0$, $t=30$ s).

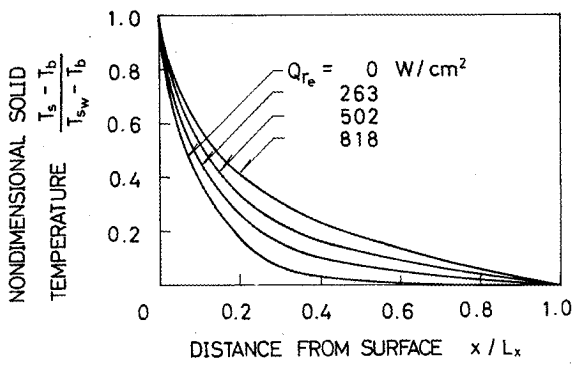

Fig. 9 Effect of incident radiative heating on in-depth temperature distribution ($m_{ref}=0.1$ g/cm^2·s, $\phi=0.66$, $Q_c=545$ W/cm^2, $y/L=0.0$, $t=30$ s).

Case 2

A radiation simulator RADON IV[16] with infrared lamps provides one-dimensional, relatively low-incident radiative heating at $Q_{r_e}=5.17$ W/cm^2 under the conditions of $Q_c=0$ W/cm^2 and $p_e=10$ N/cm^2. Since this heating condition is one-dimensional and of a factor of 50 less than that for case 1, it can hardly validate the model. However, the two-dimensional analysis can be applied to a one-dimensional case by omitting a y coordinate; and low-temperature thermal and optical properties can give qualitative information about the matrix temperature, even though the spectral radiative properties are not exactly correct. The numerical calculation was performed for the heating condition of this radiation simulator and the results were compared with the experimental data. The in-depth temperature distributions and the surface temperatures with the mass injection rate agree fairly well (see Fig. 11). In spite of several limitations in the experimental condition, the agreement tentatively confirms the feasibility of this analysis.

Conclusions

The two-dimensional unsteady material response of a transpiration-cooled system in a radiative/convective heating environment was analyzed numerically with the use of the strongly implicit procedure. The internal mass flow rate, pressure, and in-depth solid and fluid temperature distributions were obtained for various porosities and coolant mass injection rates in a CO_2/silica transpiration-cooled system. The effects of in-depth radiative transfer on such a system were discussed.

The major conclusions are as follows:

1) Increasing the incident radiative heating, while keeping the incident convective heating constant, raises the levels of the in-depth solid temperatures due to the increase of the penetrating radiative heat load.

2) The cooling effectiveness is expected to be better for lower mass injection rates and lower porosities.

3) This transpiration-cooled system seems to be feasible for a thermal protection system in a severe radiative environment.

4) The comparison with the experimental data of a one-dimensional, relatively low-incident radiative heating condition tentatively confirms the feasibility of this analysis.

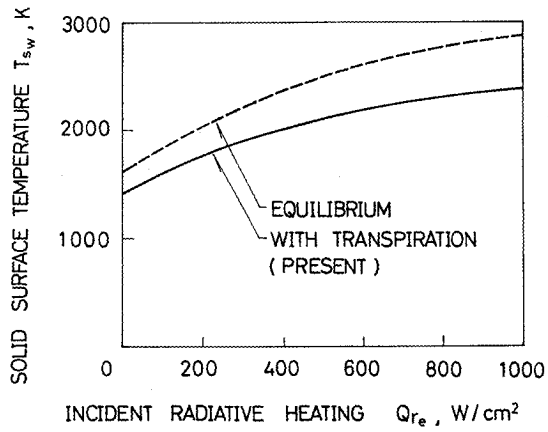

Fig. 10 Effect of incident radiative heating on solid surface temperature, same conditions as Fig. 9.

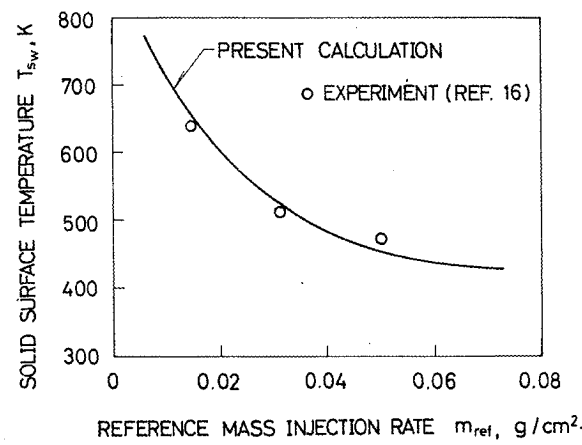

Fig. 11 Comparison of analytical results with experimental data (matrix thickness 1.0 cm, $\phi=0.37$, $t=200$ s).

Appendix

When the radiative emission inside the matrix is negligibly small compared to the radiant fluxes transmitted inward and backscattered outward, the one-dimensional radiation transfer can be described by the Kubelka-Munk "two-flux" equations[17] as

$$\frac{dI_{T_\nu}}{dx} = -(S+K)I_{T_\nu} + SI_{R_\nu} \tag{A1}$$

$$\frac{dI_{R_\nu}}{dx} = (S+K)I_{R_\nu} - SI_{T_\nu} \tag{A2}$$

where K and S are absorption and scattering coefficients, respectively, and are defined by

$$K = \phi K_f + (1-\phi)K_s \tag{A3}$$

$$S = \phi S_f + (1-\phi)S_s \tag{A4}$$

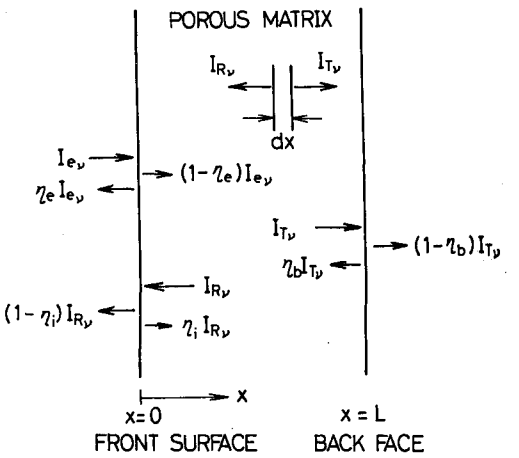

Fig. A1 Radiative transfer model.

The boundary conditions for this set of simultaneous equations (A1) and (A2) are at $x=0$ (front surface),

$$I_{T_\nu} = (1-\eta_e) I_{e_\nu} + \eta_i I_{R_\nu} \tag{A5}$$

and at $x=L_x$ (back face),

$$I_{R_\nu} = \eta_b I_{T_\nu} \tag{A6}$$

as illustrated in Fig. A1.

The general solutions are

$$I_{T_\nu} = A(1-\beta)e^{\alpha x} + B(1+\beta)e^{-\alpha x} \tag{A7}$$

$$I_{R_\nu} = A(1+\beta)e^{\alpha x} + B(1-\beta)e^{-\alpha x} \tag{A8}$$

where

$$\alpha = \sqrt{K(K+2S)}, \quad \beta = \sqrt{K/(K+2S)}$$

$$A = (1-\eta_e) I_{e_\nu} (A_0/A_1), \quad B = -(1-\eta_e) I_{e_\nu} (B_0/B_1)$$

$$A_0 = [1-\beta-\eta_b(1+\beta)]e^{-\alpha L_x}$$

$$A_1 = [(1-\beta)^2 - (1-\beta^2)(\eta_i+\eta_b) + (1+\beta)^2\eta_i\eta_b]e^{-\alpha L_x}$$
$$- [(1+\beta)^2 - (1-\beta^2)(\eta_i+\eta_b) + (1-\beta)^2\eta_i\eta_b]e^{\alpha L_x}$$

$$B_0 = (1-\beta^2)(1+\eta_b^2) - 2(1+\beta^2)\eta_b$$

$$B_1 = A_0 A_1 \tag{A9}$$

Acknowledgment

This investigation was partly supported by a Grant-in-Aid for Co-operative Research from the Ministry of Education of Japan. The authors thank T. Kurotaki for his effort in the continuous execution of the calculations.

References

[1] Moss, J. N., Anderson, E. C., and Bolz Jr., C. W., "Aerothermal Environment for Jupiter Entry Probes," AIAA Paper 76-469, July 1976; also *Progress in Astronautics and Aeronautics: Thermophysics of Spacecraft and Outer Planet Entry Probes*, Vol. 56, edited by A. E. Smith, AIAA, New York, 1977, pp. 333-354.

[2] Green, M. J. and Davy, W. C., "Galileo Probe Forebody Thermal Protection," AIAA Paper 81-1073, June 1981; also *Progress in Astronautics and Aeronautics: Thermophysics of Atmospheric Entry*, Vol. 82, edited by T. E. Horton, AIAA, New York, 1982, pp. 328-353.

[3] Kubota, H., "A Simplified Analytical Solution for Thermal Response of a One-Dimensional, Steady-State Transpiration Cooling System in Radiative and Convective Environment," NASA TN D-8129, Jan. 1976.

[4] Kubota, H., "Thermal Response of a Transpiration-Cooled System in a Radiative and Convective Environment," *Transactions of ASME, Journal of Heat Transfer*, Vol. 99, Nov. 1977, pp. 628-633.

[5] Kubota, H., "Thermal Response of an Ablation-Transpiration-Cooled System in a Radiative and Convective Environment," *Proceedings of the 12th International Symposium on Space Technology and Sciences*, Tokyo, AGNE Publishing, Inc., Tokyo, July 1977, pp. 127-132.

[6] Curry, D. M., "Two-Dimensional Analysis of Heat and Mass Transfer in Porous Media Using the Strongly Implicit Procedure," NASA TN D-7608, March 1974.

[7] Stone, H. L., "Iterative Solution of Implicit Approximations of Multidimensional Partial Differential Equations," *SIAM Journal of Numerical Analysis*, Vol. 5, Sept. 1968, pp. 530-558.

[8] Howe, J. T. and McCulley, L. D., "Volume-Reflecting Heat Shields for Entry into the Giant Planet Atmospheres," AIAA Paper 74-669, July 1974; also *Progress in Astronautics and Aeronautics: Heat Transfer with Thermal Control Applications*, Vol. 39, edited by M. M. Yovanovich, AIAA, New York, 1975, pp. 349-371.

[9] Ishii, I., "Two-Dimensional Unsteady Material Response for Transpiration Cooling System in Radiative and Convective Environment," Master Thesis, University of Tokyo, Japan, Feb. 1982.

[10] Nicolet, W. E., Howe, J. T., and Mezines, S. A., "Outer Planet Probe Entry Thermal Protection; Part II: Heat-Shielding Requirements," AIAA Paper 74-701, July 1974.

[11] Dorrance, W. H., *Viscous Hypersonic Flow*, McGraw-Hill Book Co., New York, 1962, pp. 273-315.

[12] Obert, E. F. and Gaggioli, R. A., *Thermodynamics*, McGraw-Hill Book Co., New York, 1963.

[13] Tien, C. L., "Thermal Radiation Properties of Gases," *Advances in Heat Transfer*, Vol. 5, Academic Press, New York, 1968, pp. 253-324.

[14] Curry, D. M. and Cox, J. E., "The Effect of the Porous Material Characteristics on the Internal Heat and Mass Transfer," ASME Paper 73-HT-49, Dec. 1973.

[15] Schneider, P. J., Maurer, R. E., and Strapp, M. G., "Two-Dimensional Transpiration-Cooled Nosetip," *Journal of Spacecraft and Rockets*, Vol. 8, Feb. 1971, pp. 170-176.

[16] Kubota, H., Mitsuda, M., Kurotaki, T., and Ishii, I., "Transpiration-Cooled Thermal Protection for a Relatively Low Radiation Heating," *Proceeding of the 13th International Symposium on Space Technology and Sciences*, Tokyo, July 1982, AGNE Publishing, Inc., Tokyo, pp. 593-598.

[17] Kortüm, G., *Reflectance Spectroscopy*, Springer-Verlag, New York, 1969.